Aqueductal cerebrospinal fluid pulsatility in healthy individuals is affected by impaired cerebral venous outflow

Journal:	*Journal of Magnetic Resonance Imaging*
Manuscript ID:	JMRI-13-0529.R1
Wiley - Manuscript type:	Original Research
Classification:	Clinical brain < Neuro-imaging < Clinical Science, Vascular disease < Cardiovascular and interventional imaging < Clinical Science
Manuscript Keywords:	CSF dynamics, CCSVI, aqueduct of Sylvius, cerebral venous outflow, healthy individuals, lateral ventricle volume

Aqueductal cerebrospinal fluid pulsatility in healthy individuals is affected by impaired cerebral venous outflow

Clive B. Beggs, PhD [1], Christopher Magnano, MS, [2], Simon J. Shepherd, PhD [1], Karen Marr, RVT, RDMS [2], Vesela Valnarov, MD [2], David Hojnacki, MD [3], Niels Bergsland, MS [2], Pavel Belov [2], Steven Grisafi, BS [2], Michael G. Dwyer, MS [1], Ellen Carl, PhD [1], Bianca Weinstock-Guttman, MD [3], Robert Zivadinov, MD, PhD [2,3]

[1] Medical Biophysics Laboratory, University of Bradford, Bradford, UK;
[2] Buffalo Neuroimaging Analysis Center, University at Buffalo, Buffalo, NY, USA;
[3] Jacobs MS Comprehensive and Research Center, University at Buffalo, Buffalo, NY, USA

Corresponding Author: Clive B. Beggs, PhD

Prof Clive Beggs
Centre for Infection Control and Biophysics
School of Engineering, Design & Technology
University of Bradford
Bradford
West Yorkshire
BD7 1DP
United Kingdom

email: c.b.beggs@bradford.ac.uk, Tel: +44(0)1274 233679, Fax: +44(0)1274 234124

Running title: CCSVI in healthy individuals

Abstract count: 188, Word count (text, appendix, references & tables): 5199, Number of Tables: 3, Number of Figures: 5, Number of references: 53.

Potential Conflicts of Interest

Clive B. Beggs, Christopher Magnano, Simon J. Shepherd, Karen Marr, Vesela Valnarov, Niels Bergsland, Pavel Belov, Steven Grisafi, Michael G. Dwyer and Ellen Carl have nothing to disclose. Bianca Weinstock-Guttman received personal compensation for consulting, speaking, and serving on a scientific advisory board for Biogen Idec, Teva Neuroscience, and EMD Serono. Dr. Weinstock-Guttman also received financial support for research activities from NMSS, NIH, ITN, Teva Neuroscience, Biogen Idec, EMD Serono, and Aspreva. David Hojnacki has received speaker honoraria and consultant fees from Biogen Idec, Teva Pharmaceutical Industries Ltd., EMD Serono, Pfizer Inc, and Novartis. Robert Zivadinov received personal compensation from Teva Pharmaceuticals, Biogen Idec, EMD Serono and Genzyme for speaking and consultant fees. Dr. Zivadinov received financial support for research activities from Biogen Idec, Teva Pharmaceuticals, Genzyme and Novartis.

Grant Support

This work has been supported in part by grants from the Annette Funicello Research Fund for Neurological Diseases and Jacquemin Family Foundation.

Aqueductal cerebrospinal fluid pulsatility in healthy individuals is affected by impaired cerebral venous outflow

Abstract

Purpose: To investigate cerebrospinal fluid (CSF) dynamics in the aqueduct of Sylvius (AoS) in chronic cerebrospinal venous insufficiency (CCSVI) positive and negative healthy individuals using cine phase contrast imaging.

Materials and Methods: Fifty one healthy individuals [32 CCSVI negative and 19 age-matched CCSVI positive subjects] were examined using Doppler sonography (DS). Diagnosis of CCSVI was established if subjects fulfilled ≥2 venous hemodynamic criteria on DS. CSF flow and velocity measures were quantified using a semi-automated method and compared with clinical and routine 3T MRI outcomes.

Results: CCSVI was associated with increased CSF pulsatility in the AoS. Net positive CSF flow was 32% greater in the CCSVI positive group compared with the CCSVI negative group (p=0.008). This was accompanied by a 28% increase in the mean aqueductal characteristic signal (i.e. the AoS cross-sectional area over the cardiac cycle) in the CCSVI positive group compared with the CCSVI negative group (p=0.021).

Conclusion: CSF dynamics are altered in CCSVI positive healthy individuals, as demonstrated by increased pulsatility. This is accompanied by enlargement of the AoS, suggesting that structural changes may be occurring in the brain parenchyma of CCSVI positive healthy individuals.

Keywords: CSF dynamics, CCSVI, cerebral venous outflow, aqueduct of Sylvius, healthy individuals, lateral ventricle volume

Introduction

Recently it has been suggested that abnormalities of the venous system might be associated with multiple sclerosis (MS) (1-5). This has led some to postulate the concept of chronic cerebrospinal venous insufficiency (CCSVI) as an indicator of neurovascular pathology. However, a number of studies have shown that CCSVI also occurs in healthy individuals with unknown pathology (4,6,7), leading many to question its validity (8-13). Criticism has been levelled at the concept of CCSVI because it implies an abnormal cerebral venous drainage system. In reality, humans exhibit great variability in the venous system, making it difficult to differentiate what is normal from what is abnormal (14,15). Hydrodynamic analysis of the cerebral venous outflow has shown that patients with MS exhibit increased hydraulic resistance to extracranial venous blood flow compared with healthy controls (16,17). Furthermore, several studies have shown that MS is associated with increased cerebrospinal fluid (CSF) pulsatility in the aqueduct of Sylvius (AoS) (18-20). Although Zamboni et al (19) observed increased CSF pulsatility in MS patients diagnosed with CCSVI, it is not known if the two phenomena are linked. Indeed, it may be that increased CSF pulsatility in MS patients is primarily due to ventricular enlargement associated with brain atrophy (21,22).

In a similar manner to individuals with MS, patients with normal pressure hydrocephalus (NPH) appear to exhibit increased AoS pulsatility (23-28). Given that NPH is thought to be associated with venous hypertension in the dural sinuses (29,30), it may be that impaired cerebral venous outflow alters the dynamics of the intracranial CSF system, irrespective of any pathology. In

order to test this hypothesis, we undertook a study involving 51 age-matched healthy individuals with no family history of MS. The aim of the study was simply to evaluate whether or not CCSVI is associated with changes in the dynamics of the intracranial CSF system in healthy individuals without any known neurological condition.

Materials and methods

Patient population

Fifty one healthy individuals [32 CCSVI negative and 19 CCSVI positive] were enrolled in this study. They were part of a larger study that investigated the relationship between CCSVI and conventional MRI characteristics in MS patients and healthy individuals (31). Inclusion criteria were: age 18 to 75 years, undergoing Doppler sonography (DS) and MRI scan with cine phase contrast imaging for CSF flow estimation. Relevant information relating to: vascular risk factors [body mass index (BMI), hypertension, heart disease and smoking] was also collected. The individuals also needed to qualify on a health screening questionnaire containing information about medical history (illnesses, surgeries, medications, etc.) and meet the health screen requirements for MRI on physical examination, as previously described (4,31,32). Exclusion criteria were: pre-existing medical conditions known to be associated with brain pathology (e.g. cerebrovascular disease, positive history of alcohol abuse, etc.), history of cerebral congenital vascular malformations, type 1 diabetes, or pregnancy.

All participants underwent clinical, DS and MRI examinations. The study was approved by the local Institutional Review Board and informed consent was obtained from all subjects.

Doppler sonography

Extra- and trans-cranial DS was performed on a color-coded DS scanner (MyLab 25; Esaote-Biosound, Irvine, California) equipped with a 5.0- to 10-Mhz transducer to examine venous return in the internal jugular veins (IJVs) and vertebral veins (VVs). The DS examination was performed by 2 trained technologists who were blinded to the subjects' characteristics. The detailed scanning protocol and validation were recently reported (4,33). Briefly, the following 5 VH (venous hemodynamic) parameters indicative of CCSVI were investigated: 1) Reflux/bidirectional flow in the IJVs and/or in the VVs in sitting and in supine positions, defined as flow directed towards the brain for a duration of >0.88 s; 2) Reflux/bidirectional flow in the deep cerebral veins defined as reverse flow for a duration of 0.5 s in one of the intra-cranial veins; 3) B-mode abnormalities or stenoses in IJVs. IJV stenosis is defined as a cross-sectional area (CSA) of this vein ≤0.3 cm^2; 4) Flow that is not Doppler-detectable in IJVs and/or VVs despite multiple deep breaths, and 5) Reverted postural control of the main cerebral venous outflow pathway by measuring the difference of the CSA of the IJVs in the supine and upright positions. A subject was considered CCSVI-positive if ≥2 VH criteria were fulfilled, as previously proposed (1). We also calculated the VH insufficiency severity score (VHISS) as a measure of CCSVI severity (19). The overall VHISS score

is the weighted sum of the scores contributed by each individual VH criterion (i.e. VHISS = VHISS1 + VHISS2 + VHISS3 + VHISS4 + VHISS5). The VHISS score is an ordinal measure of the overall extent and number of VH flow pattern anomalies, with a higher value of VHISS indicating a greater severity of VH flow pattern anomalies. The minimum possible VHISS value is 0 and the maximum 16.

MRI acquisition and analysis

All subjects were examined on a 3 Tesla GE Signa Excite HD 12.0 Twin Speed scanner (General Electric, Milwaukee, WI). All sequences were run on an 8-channel head and neck (HDNV) coil. All analyses were performed in a blinded manner.

MRI sequences included 3D high resolution (HIRES) T1-WI using a fast spoiled gradient echo (FSPGR) with magnetization-prepared inversion recovery (IR) pulse and cine phase contrast imaging for CSF flow estimation. Pulse sequence characteristics for 3D T1 sequence were: a 256 x 256 matrix and a 25.6 cm field of view (FOV) for an in-plane resolution of 1 x 1 mm2 with a phase FOV (pFOV) of 75% and one average. Sequence specific parameters were: 1-mm thick slices with no gap, echo time/inversion time/repetition time (TE/TI/TR)=2.8/900/5.9 ms, flip angle (FA)=10°. On 3D t1, the SIENAX cross-sectional software tool (version 2.6; http://fsl.fmrib.ox.ac.uk/fsl/fslwiki/SIENA) was used to estimate normalized brain volume (NBV) and normalized lateral ventricular volume (NLVV), as

previously described (34). Prior to segmentation, the 3D T1 WI was modified using an in-house developed inpainting tool to avoid the impact of T1 hypointensities.

CSF flow quantification was performed using a single slice cine phase-contrast velocity-encoded pulse-gated gradient echo sequence (cine PC) with an TE/TR of 7.9/40 ms, a slice thickness of 4 mm, a velocity encoding of 20 cm/s, and 32 phases acquired corresponding to the cardiac cycle (18). Other relevant scan parameters included a FA of 20°, FOV 10.0 cm, and a phase FOV of 100%. A sagittal T2-weighted fast SE sequence was also acquired as a localizer for the cine PC prescription, as previously described, with the cine PC sequence prescribed as an oblique axial slice through the AoS (18). All subjects underwent the MRI exam during the same time of day (in the afternoon hours) to control for circadian variation. The cine PC sequence was acquired with the AoS in the center of the FOV, such that the wrap around artifact was present in the edges of the FOV, but did not overlap with the desired ROI. To ensure reproducibility, repeat scans were performed as described in Magnano et al (18).

Cine phase contrast image analysis

The net positive and net negative flows (NPF and NNF), together with the net flow (NF = NNF + NPF) were calculated, as previously described (18). Briefly, CSF flow data was processed using GE ReportCard software (version 3.6;

General Electric, GE, Milwaukee, WI) and positive and negative velocities over all 32 phases were recorded. A semi-automated minimum area of contour change (MACC) program was used to correct the ROIs for each phase, as previously described (18). MACC automatically determined the edges of an ROI by selecting a surrounding iso-contour curve which marks the steepest overall gradient of image intensity values, with sub-voxel accuracy. NPF and NNF were calculated using only the phases which have positive and negative velocities, respectively (18). The respective CSF flow rates were calculated by multiplying the measured CSF velocities by the measured CSA of the AoS over the cardiac cycle. CSF flow measures are presented in microliters per beat (μL/beat, 1μL = 1mm^3), while CSF velocity measures are presented in cm/s. CSF flow direction was calculated based on slice prescription such that flow through the AoS out of the slice (during diastole, towards the third ventricle) was given as positive, whereas flow into the slice (during systole, towards the fourth ventricle) was negative, as described previously (18).

Statistical analysis

Analysis was undertaken using the Statistical Package for Social Sciences (SPSS, IBM, Armonk, New York, USA) and in-house algorithms written in Matlab (Mathworks, Natick, Mass). The demographic and clinical differences between the CCSVI positive and negative groups were tested using the chi-square test and Student's t-test, while analysis of the MRI data was undertaken using the Mann–Whitney rank sum test. CSF flow differences

between the study groups were evaluated using the Mann–Whitney rank sum test. In order to assess the impact of a CCSVI diagnosis on aqueductal behavior, for each subject we divided the sequential CSF flow signal by the sequential CSF velocity signal, to produce the aqueductal characteristic signal (ACS), shown in Figure 3, which represents the changes in the AoS cross-sectional area throughout the cardiac cycle. This is identical to the cross sectional area of the AoS as calculated by MACC at each instantaneous phase of the cardiac cycle. Values of $p<0.05$ using a two-tailed test were considered statistically significant after the Benjamini-Hochberg (35) correction for multiple comparisons was applied.

The following analysis techniques were also employed:

1. Correlation matrices (Pearson's r) were computed for the CCSVI positive and negative groups, to identify changes in the relationships between the variables within the dataset. Statistical significance was determined using a two-tailed Fisher r-to-z transformation.
2. Singular value decomposition (SVD) analysis was used to visualize the differences between the CCSVI positive and negative groups, and also to generate sensitivity and specificity scores.

In order to perform singular value decomposition (SVD) the data, we created a ($m \times 3$) matrix, $\boldsymbol{Z}$, containing the data for both the CCSVI negative and positive groups. The columns of the $\boldsymbol{Z}$ matrix comprised the variables NNF,

NPF and NLVV, which we mean-adjusted and standardized to unit variance. SVD was then performed on ***Z*** as follows:

$$Z = U.S.V^T \quad (1)$$

where: ***U*** is a (m × 3) left singular vector (LSV) matrix with identical dimensions to ***Z***; ***S*** is a (3 × 3) singular value (SV) matrix; and ***V*** is a (3 × 3) right singular vector (RSV) matrix. In ***U***, the columns (LSVs) are orthogonal composites of the three original variables in ***Z***, with the rows equating to the participants in the study. Plotting the individual LSVs against each other produced scatter plots of the orthogonalized data. By identifying the elements of *U* that belong to the CCSVI negative and positive cohorts, respectively, it was possible to perform cluster analysis.

Results

Demographic and clinical characteristics

Table 1 shows demographic, clinical and conventional MRI characteristics of the CCSVI positive and negative groups. There were no significant age- or sex- differences between the CCSVI positive and negative subjects, with no significant difference between the NBV. No significant differences were found between the two groups regarding: BMI; hypertension; heart problems; and smoking habit. There were however significant differences for VH criteria score ($p<0.0001$) and VHISS score ($p<0.0001$) between the CCSVI positive and negative cohorts.

Time series analysis

Figures 1 and 2 present average time series signals for CSF flow and velocity in the AoS over a cardiac cycle. From these it can be seen that the CCSVI positive individuals exhibit increased pulsatility, in both the flow and velocity signals. While there was no significant difference between the CSF velocity signals for the two groups, the peak positive flow rate (towards the lateral ventricles) was significantly greater ($p=0.023$) in the CCSVI positive group compared with the negative group. Similarly, the mean ACS signal, shown in Figure 3, was significantly greater ($p=0.021$) in the CCSVI positive group compared with the negative group.

Univariate analysis

Table 2 shows the quantitative assessment and univariate analysis results for the respective MRI variables, with the subjects grouped according to CCSVI status. This reveals that although NLVV was increased in the CCSVI positive group, this increase was not significant. A statistically significant 32% increase in CSF NPF towards the lateral ventricles ($p=0.008$) was observed in the CCSVI positive group. A similar increase was observed in NNF towards the spine in the CCSVI positive individuals, but this did not reach significance. Likewise, the decrease in CSF NF in the CCSVI positive individuals did not reach significance. The 28% increase in the mean ACS value ($p=0.021$) in the CCSVI positive group compared with the CCSVI negative group was significant.

Correlation analysis

Correlation analysis of the MRI data revealed that associations between NLVV and the CSF related variables in CCSVI positive subjects were generally weaker then in CCSVI negative subjects. For example, Figure 4 presents a scatter plot of NNF verses NLVV, which in the CCSVI negative group exhibited a relatively strong negative correlation ($r=-0.686$, $p<0.001$), but was lost in the CCSVI positive group ($r=-0.103$, $p=0.674$) – a change that was significant using a Fisher transformation ($p=0.018$). Likewise, the strong positive correlations between the variables NPF and NLVV ($r=0.761$, $p<0.001$), and ACS and NLVV ($r=0.720$, $p<0.001$) in the CCSVI negative group were weaker in the positive group ($r=0.404$, $p=0.086$ and $r=0.454$, $p=0.051$). However, these changes were not significant.

No significant correlation was observed between VHISS score and any of the MRI variables for either group, or indeed when both groups were aggregated together.

Singular value decomposition cluster analysis

SVD analysis was performed using just three variables NNF, NPF and NLVV (being a derived variable, NF was excluded from the SVD analysis). The results of this analysis are presented in Figure 5, which shows a plot of the first LSV against the third LSV. The LSVs are composite variables derived from the original variables, which have been orthogonalized. This analysis separates the CCSVI positive and negative groups relatively well, although

there is some overlap. The two groups can be broadly separated by the straight-line equation:

$$LSV3 = (2.6 \times LSV1) + 0.04 \quad (2)$$

Separating the groups using this equation yields sensitivity and specificity scores of 73.7% and 71.9% respectively (p=0.025). The singular values associated with the first, second and third LSVs were 11.008, 5.058 and 1.800 respectively. This indicates that the first LSV explains 80.8% of the variance in the system, while the second and third LSVs explain 17.0% and 2.2% of the variance, respectively. The composition of the various LSVs is presented in Table 3, which shows the linear coefficients that must be applied to the each variable in order to reconstruct the respective LSVs. From this it can be seen that the coefficients relating to variables NNF and NPF are more dominant in the first and third LSVs, whereas the coefficient relating to NLVV is more dominant in the second LSV.

Discussion

The subject of CCSVI has been mired with controversy (8,36), with many researchers doubting that it is indicative of any pathology (8-13). However, there is growing evidence that restricted cerebral venous outflow is a phenomenon that is more prevalent in patients with MS, (1-3,5,37), even though it is also observed in both healthy individuals (4,6,7) and those with other neurological disease (4). While the reasons for this are unclear, it has

been shown using cervical plethysmography (16,17) that MS patients diagnosed with CCSVI exhibit on average a 63.5% increase in the hydraulic resistance of the venous pathways from the brain to the heart compared with CCSVI negative healthy controls. As such, it raises intriguing questions as to whether the increase in aqueductal CSF pulsatility observed in MS patients (19) is associated with MS or CCSVI. If increased CSF pulsatility were purely an attribute of MS, then one would not expect the phenomenon to be present in CCSVI positive healthy controls.

In an attempt to answer the above question, we undertook the present study, with the aim of establishing whether or not CCSVI is associated with altered intracranial CSF dynamics in healthy individuals with no known neurological pathology. From the results in Table 2 and figures 1-3 it appears that CCSVI is associated with changes in the aqueductal CSF flow dynamics in healthy individuals. In particular, NPF was significantly increased ($p=0.008$) in the CCSVI positive group compared with the CCSVI negative group. NNF was also increased, but this was not significant. Likewise, NF decreased in the CCSVI positive group, but this was not significant. Comparison between the aqueductal CSF flow curves published by Magnano et al (18) for both MS patients and healthy controls reveals similar curves to those for the healthy CCSVI positive and negative subjects in the present study, suggesting that increased aqueductal pulsatility may be primarily associated with impaired cerebral venous drainage rather than MS itself. Indeed, the fact that we found greatly increased NPF in CCSVI positive healthy individuals, just as Zamboni et al (19), Gorucu et al (20), Magnano et al (18) all observed in MS patients,

further implies that the phenomenon may be biomechanical in nature, rather than due to neuronal damage/brain atrophy.

Being encased in a rigid enclosure, the brain employs a complex intracranial fluid regulatory mechanism to compensate for increased blood flow during systole. This system compensates for the transient increase in arterial blood entering the cranium during systole, by displacing an approximately equal volume of CSF through the foramen magnum into the spinal column (38). It does this by employing a sophisticated windkessel mechanism to smooth blood flow through the cerebral capillary bed (39,40); something that appears to be sensitive to changes in the cerebral venous system (41-43). Indeed, it has been postulated that the venous system plays an important role in regulating the dynamics of the intracranial fluid system (44). While the mechanisms involved are poorly understood, it can be hypothesized that impairment of cerebral venous outflow is likely to induce retrograde hypertension in the dural sinuses, as Zamboni et al (45) observed; something that might reduce intracranial compliance resulting in altered CSF behaviour (43). Evidence supporting this model comes from Luetmer et al (23), Schroth & Klose (24), Gideon et al (25), Kim et al (26), El Sankari et al (27) and Bradley (28), all of whom found CSF pulsatility in the AoS to be markedly greater in NPH patients compared with controls. Given that reduced intracranial compliance (29,30,46,47), induced by venous hypertension, is thought to be involved in NPH (29,30,48,49), this suggests that impaired venous outflow is capable of altering the intracranial CSF dynamics, just as we observed in the CCSVI positive healthy individuals. Further evidence to

support this opinion comes from an interventional study by Zivadinov et al (50) in which percutaneous transluminal venous angioplasty was shown to reduce aqueductal CSF pulsatility in MS patients diagnosed with CCSVI. Although abnormal CSF dynamics and their relation to health verses disease status is beyond the scope of this article, it is noticeable that their role in neurodegenerative disease is becoming increasingly contemplated (51).

One interesting finding of our study was that CCSVI appeared to be associated with a weakening in the correlation between the aqueductal CSF pulse variables and NLVV. In healthy individuals there is normally a strong correlation between lateral ventricle size and aqueductal CSF flow (52). However, in the CCSVI positive group we found the correlations between NNF, NPF, ACS and NLVV to be markedly weaker than that in the CCSVI negative group. While the reasons for this are not understood, it may be that structural changes are at work. Evidence supporting this opinion comes from the ensemble mean ACS over the cardiac cycle. This signal is derived by dividing each CSF flow signal, by the corresponding CSF velocity signal and therefore represents the changes in the AoS area throughout the cardiac cycle. The mean ACS is significantly different in both groups, with the mean aqueductal area being substantially larger in the CCSVI positive group compared with the CCSVI negative group. From this it can be concluded that the increased CSF pulsatile flow in the CCSVI positive group is facilitated more by enlargement of the AoS than any increase in CSF velocity.

This study is not without limitations. First, the number of the enrolled healthy individuals was relatively small and therefore further studies should extend our findings using a larger sample size. Second, the diagnosis of CCSVI was established only by using DS, while recent studies suggest that increased sensitivity and specificity of CCSVI diagnosis, can be achieved using a variety of non-invasive and invasive imaging approaches (53). Lastly, the effect of altered CSF pulsatility on long-term neurologic outcomes is unknown, and only longitudinal studies will be able to provide further insight on this important question.

In conclusion, the results of the study suggest that CCSVI is associated with intracranial biomechanical changes in healthy individuals. Indeed, such was the magnitude of the changes observed that it was relatively easy to discriminate, using SVD analysis, between the CCSVI positive and negative groups using just the three variables NNF, NPF and NLVV. Given that impaired cerebral venous outflow has been shown to be associated with MS (16,17), this implies that similar changes in intracranial CSF dynamics observed in MS patients (18-20), might be primarily due to the presence of CCSVI rather than due to neuronal damage.

References

1. Zamboni P, Galeotti R, Menegatti E, et al. Chronic cerebrospinal venous insufficiency in patients with multiple sclerosis. J Neurol Neurosurg Psychiatry 2009;80(4):392-399.
2. Simka M, Kostecki J, Zaniewski M, Majewski E, Hartel M. Extracranial Doppler sonographic criteria of chronic cerebrospinal venous insufficiency in the patients with multiple sclerosis. Int Angiol 2010;29(2):109-114.
3. Al-Omari MH, Rousan LA. Internal jugular vein morphology and hemodynamics in patients with multiple sclerosis. Int Angiol 2010;29(2):115-120.
4. Zivadinov R, Marr K, Cutter G, et al. Prevalence, sensitivity, and specificity of chronic cerebrospinal venous insufficiency in MS. Neurology 2011;77(2):138-144.
5. Zivadinov R, Galeotti R, Hojnacki D, et al. Value of MR Venography for Detection of Internal Jugular Vein Anomalies in Multiple Sclerosis: A Pilot Longitudinal Study. AJNR Am J Neuroradiol;32(5):938-946.
6. Wattjes MP, van Oosten BW, de Graaf WL, et al. No association of abnormal cranial venous drainage with multiple sclerosis: a magnetic resonance venography and flow-quantification study. J Neurol Neurosurg Psychiatry 2011;82(4):429-435.
7. Centonze D, Floris R, Stefanini M, et al. Proposed chronic cerebrospinal venous insufficiency criteria do not predict multiple sclerosis risk or severity. Ann Neurol 2011;70(1):51-58.

8. Doepp F, Paul F, Valdueza JM, Schmierer K, Schreiber SJ. No cerebrocervical venous congestion in patients with multiple sclerosis. Ann Neurol 2010;68(2):173-183.

9. Doepp F, Wurfel JT, Pfueller CF, et al. Venous drainage in multiple sclerosis: a combined MRI and ultrasound study. Neurology 2011;77(19):1745-1751.

10. Mayer CA, Pfeilschifter W, Lorenz MW, et al. The perfect crime? CCSVI not leaving a trace in MS. J Neurol Neurosurg Psychiatry 2011;82(4):436-440.

11. Khan O, Filippi M, Freedman MS, et al. Chronic cerebrospinal venous insufficiency and multiple sclerosis. Ann Neurol 2010;67(3):286-290.

12. Wattjes MP, Doepp F, Bendszus M, Fiehler J. ["Chronic cerebrospinal venous insufficiency" in multiple sclerosis - is multiple sclerosis a disease of the cerebrospinal venous outflow system?]. Rofo 2011;183(6):523-530.

13. Baracchini C, Atzori M, Gallo P. CCSVI and MS: no meaning, no fact. Neurol Sci 2012.

14. Beards SC, Yule S, Kassner A, Jackson A. Anatomical variation of cerebral venous drainage: the theoretical effect on jugular bulb blood samples. Anaesthesia 1998;53(7):627-633.

15. Schummer W, Schummer C, Bredle D, Frober R. The anterior jugular venous system: variability and clinical impact. Anesth Analg 2004;99(6):1625-1629, table of contents.

16. Zamboni P, Menegatti E, Conforti P, Shepherd S, Tessari M, Beggs C. Assessment of cerebral venous return by a novel plethysmography method. J Vasc Surg 2012;56:677-685.

17. Beggs C, Shepherd S, Zamboni P. Cerebral venous outflow resistance and interpretation of cervical plethysmography data with respect to the diagnosis of chronic cerebrospinal venous insufficiency. Phlebology 2012;DOI: 10.1258/phleb.2012.012039:1-9.

18. Magnano C, Schirda C, Weinstock-Guttman B, et al. Cine cerebrospinal fluid imaging in multiple sclerosis. J Magn Reson Imaging 2012;36:825-834.

19. Zamboni P, Menegatti E, Weinstock-Guttman B, et al. The severity of chronic cerebrospinal venous insufficiency in patients with multiple sclerosis is related to altered cerebrospinal fluid dynamics. Funct Neurol 2009;24(3):133-138.

20. Gorucu Y, Albayram S, Balci B, et al. Cerebrospinal fluid flow dynamics in patients with multiple sclerosis: a phase contrast magnetic resonance study. Funct Neurol 2011;26(4):215-222.

21. Dalton CM, Brex PA, Jenkins R, et al. Progressive ventricular enlargement in patients with clinically isolated syndromes is associated with the early development of multiple sclerosis. J Neurol Neurosurg Psychiatry 2002;73(2):141-147.

22. Dalton CM, Miszkiel KA, O'Connor PW, Plant GT, Rice GP, Miller DH. Ventricular enlargement in MS: one-year change at various stages of disease. Neurology 2006;66(5):693-698.

23. Luetmer PH, Huston J, Friedman JA, et al. Measurement of cerebrospinal fluid flow at the cerebral aqueduct by use of phase-contrast magnetic resonance imaging: technique validation and utility in diagnosing idiopathic normal pressure hydrocephalus. Neurosurgery 2002;50(3):534-543; discussion 543-534.

24. Schroth G, Klose U. Cerebrospinal fluid flow. III. Pathological cerebrospinal fluid pulsations. Neuroradiology 1992;35(1):16-24.

25. Gideon P, Stahlberg F, Thomsen C, Gjerris F, Sorensen PS, Henriksen O. Cerebrospinal fluid flow and production in patients with normal pressure hydrocephalus studied by MRI. Neuroradiology 1994;36(3):210-215.

26. Kim DS, Choi JU, Huh R, Yun PH, Kim DI. Quantitative assessment of cerebrospinal fluid hydrodynamics using a phase-contrast cine MR image in hydrocephalus. Childs Nerv Syst 1999;15(9):461-467.

27. El Sankari S, Gondry-Jouet C, Fichten A, et al. Cerebrospinal fluid and blood flow in mild cognitive impairment and Alzheimer's disease: a differential diagnosis from idiopathic normal pressure hydrocephalus. Fluids Barriers CNS 2011;8(1):12.

28. Bradley WG, Jr., Scalzo D, Queralt J, Nitz WN, Atkinson DJ, Wong P. Normal-pressure hydrocephalus: evaluation with cerebrospinal fluid flow measurements at MR imaging. Radiology 1996;198(2):523-529.

29. Bateman GA. Vascular compliance in normal pressure hydrocephalus. AJNR Am J Neuroradiol 2000;21(9):1574-1585.

30. Bateman GA. The pathophysiology of idiopathic normal pressure hydrocephalus: cerebral ischemia or altered venous hemodynamics? AJNR Am J Neuroradiol 2008;29(1):198-203.

31. Zivadinov R, Cutter G, Marr K, et al. No Association Between Conventional Brain MR Imaging and Chronic Cerebrospinal Venous Insufficiency in Multiple Sclerosis. AJNR Am J Neuroradiol 2012.

32. Dolic K, Weinstock-Guttman B, Marr K, et al. Risk factors for chronic cerebrospinal venous insufficiency (CCSVI) in a large cohort of volunteers. PLoS One 2011;6(11):e28062.

33. Dolic K, Marr K, Valnarov V, et al. Sensitivity and specificity for screening of chronic cerebrospinal venous insufficiency using a multimodal non-invasive imaging approach in patients with multiple sclerosis. Funct Neurol 2011;26(4):205-214.

34. Zivadinov R, Heininen-Brown M, Schirda CV, et al. Abnormal subcortical deep-gray matter susceptibility-weighted imaging filtered phase measurements in patients with multiple sclerosis: a case-control study. Neuroimage 2012;59(1):331-339.

35. Benjamini Y, Hochberg Y. Controlling the false discovery rate: a practical and powerful approach to multiple testing. Journal of the Royal Statistical Society B 1995;57(1):289-300.

36. Beggs C. Multiple sclerosis appears to be associated with cerebral venous abnormalities. Ann Neurol 2010;68(4):560-561.

37. Zivadinov R, Marr K, Cutter G, et al. Prevalence, sensitivity, and specificity of chronic cerebrospinal venous insufficiency in MS. Neurology 2011;77:138-144.

38. Egnor M, Zheng L, Rosiello A, Gutman F, Davis R. A model of pulsations in communicating hydrocephalus. Pediatr Neurosurg 2002;36(6):281-303.

39. Bateman GA, Levi CR, Schofield P, Wang Y, Lovett EC. The venous manifestations of pulse wave encephalopathy: windkessel dysfunction in normal aging and senile dementia. Neuroradiology 2008;50(6):491-497.

40. Bateman GA. Pulse-wave encephalopathy: a comparative study of the hydrodynamics of leukoaraiosis and normal-pressure hydrocephalus. Neuroradiology 2002;44(9):740-748.

41. Bateman GA. Magnetic resonance imaging quantification of compliance and collateral flow in late-onset idiopathic aqueductal stenosis: venous pathophysiology revisited. J Neurosurg 2007;107(5):951-958.

42. Bateman GA. Arterial inflow and venous outflow in idiopathic intracranial hypertension associated with venous outflow stenoses. J Clin Neurosci 2008;15(4):402-408.

43. Beggs CB. Venous Haemodynamics in Neurological Disorders: An Analytical Review with Hydrodynamic Analysis. BMC Medicine. BMC Med (in press).

44. El Sankari S, Czosnyka M, Lehmann P, Meyer ME, Deramond H, Baledent O. Cerebral Blood and CSF Flow Patterns in Patients Diagnosed for Cerebral Venous Thrombosis - An Observational Study. J Clin Imaging Sci 2012;2:41.

45. Zamboni P, Galeotti R, Menegatti E, et al. A prospective open-label study of endovascular treatment of chronic cerebrospinal venous insufficiency. J Vasc Surg 2009;50(6):1348-1358 e1341-1343.

46. Miyati T, Mase M, Kasai H, et al. Noninvasive MRI assessment of intracranial compliance in idiopathic normal pressure hydrocephalus. J Magn Reson Imaging 2007;26(2):274-278.

47. Mase M, Miyati T, Kasai H, et al. Noninvasive estimation of intracranial compliance in idiopathic NPH using MRI. Acta Neurochir Suppl 2008;102:115-118.

48. Williams H. The venous hypothesis of hydrocephalus. Med Hypotheses 2008;70(4):743-747.

49. Williams H. A unifying hypothesis for hydrocephalus, Chiari malformation, syringomyelia, anencephaly and spina bifida. Cerebrospinal Fluid Res 2008;5:7.

50. Zivadinov R, Magnano C, Galeotti R, et al. Changes of Cine Cerebrospinal Fluid Dynamics in Patients with Multiple Sclerosis Treated with Percutaneous Transluminal Angioplasty: Case-control Study. J Vasc Interv Radiol 2013;24(6):829-838.

51. Nedergaard M. Neuroscience. Garbage truck of the brain. Science 2013;340(6140):1529-1530.

52. Zhu DC, Xenos M, Linninger AA, Penn RD. Dynamics of lateral ventricle and cerebrospinal fluid in normal and hydrocephalic brains. J Magn Reson Imaging 2006;24(4):756-770.

53. Dolic K, Siddiqui AH, Karmon Y, Marr K, Zivadinov R. The role of noninvasive and invasive diagnostic imaging techniques for detection

of extra-cranial venous system anomalies and developmental variants. BMC Med 2013;11:155.

Tables

Table 1. Demographic, clinical and whole brain volume characteristics in healthy CCSVI positive and negative individuals.

	CCSVI negative (n = 32)	CCSVI positive (n = 19)	Significance (p value)
Female gender, n (%)	21 (65.6)	9 (47.4)	0.200
Age in years, mean (SD)	44.3 (14.8)	44.5 (19.1)	0.967
BMI, mean (SD)	25.7 (5.3)	27.1 (5.3)	0.317
Hypertension, n (%)	2 (6.3)	0 (0.0)	0.266
Heart Disease, n (%)	5 (15.6)	2 (10.5)	0.609
Current Smokers, n (%)	3 (15.0)	0 (0.0)	0.143
Ever Smokers, n (%)	13 (65.0)	6 (13.0)	0.285
Type 1 Diabetes, n (%)	0 (0.0)	0 (0.0)	1.000
VH criteria score, mean (SD)	0.66 (0.48)	2.37 (0.60)	<0.001
VHISS score, mean (SD)	1.31 (1.06)	4.42 (1.43)	<0.001
NBV, mean (SD)	1531.4 (86.0)	1509.2 (74.8)	0.340

CCSVI - chronic cerebrospinal venous insufficiency; BMI – body mass index; VH – venous hemodynamic; VHISS – venous hemodynamic insufficiency severity score; NBV – normalized brain volume.

The differences between the study groups were tested using the student's t-test and chi-square test.

Table 2. MRI characteristics in healthy individuals.

	CCSVI Negative (n = 32)	CCSVI Positive (n = 19)	Significance (p value)	Effect Size Cohen's d
NNF (μL/beat), mean (SD)	-27.6 (19.5)	-33.3 (16.9)	0.092	0.304
NPF (μL/beat), mean (SD)	23.6 (22.0)	31.2 (13.6)	0.008	0.391
NF (μL/beat), mean (SD)	-4.0 (7.5)	-2.1 (8.9)	0.080	0.245
Mean ACS ($mm^{2)}$, mean (SD)	1.0 (0.5)	1.3 (0.5)	0.021	0.585
NLVV (mL), mean (SD)	37.5 (21.5)	44.1 (18.3)	0.147	0.322

CCSVI - chronic cerebrospinal venous insufficiency; NNF – net negative CSF flow; NPF – net positive CSF flow; NF – net CSF flow (i.e. NNF+NPF); NLVV – normalized lateral ventricle volume.

The differences between the study groups were tested using the Mann-Whitney U-test, and Cohen's d test.

Table 3. Composition of respective left singular vectors (LSVs) used in the singular value decomposition (SVD).

	NNF	NPF	NLVV
First LSV	0.0566	-0.0535	0.0467
Second LSV	-0.0402	0.1015	0.1648
Third LSV	-0.4194	-0.3468	0.1113

NNF – net negative CSF flow; NPF – net positive CSF flow; NLVV – normalized lateral ventricle volume.

NB. The values in the table are the linear coefficients that must be applied to the component variables in order to reconstruct the respective LSVs.

Figure Captions

Figure 1. Ensemble mean aqueductal CSF flow signal over a cardiac cycle for both the CCSVI positive and negative groups. Between groups difference in positive amplitude (p=0.023) and negative amplitude (p=0.044). The phases of cycle where the difference between the signals is significant (p<0.050) are 8-14, 21 and 26-32. (Error bars represent one standard deviation.)

Figure 2. Ensemble mean aqueductal CSF velocity signal over a cardiac cycle for both the CCSVI positive and negative groups. Between groups difference in positive amplitude (p=0.136) and negative amplitude (p=0.316). A statistically significant difference between the signals (p<0.050) is only observed for phase 32 of the cycle. (Error bars represent one standard deviation.)

Figure 3. Sequential ensemble mean ACS over a cardiac cycle for both the CCSVI positive and negative groups. Between groups mean ACS, p=0.021. The phases of cycle where the difference between the signals is significant (p<0.050) are 8-10, 14-15, 18-28 and 30-32. (Error bars represent one standard deviation.)

Figure 4. Scatter plot of NNF verses NLVV for the CCSVI positive and negative groups. CCSVI negative group (r=-0.686; p<0.001) and CCSVI positive group (r=-0.103; p=0.674).

Figure 5. Singular value decomposition (SVD) cluster analysis results (derived using the three variables NNF, NPF and NLVV) (p=0.025).

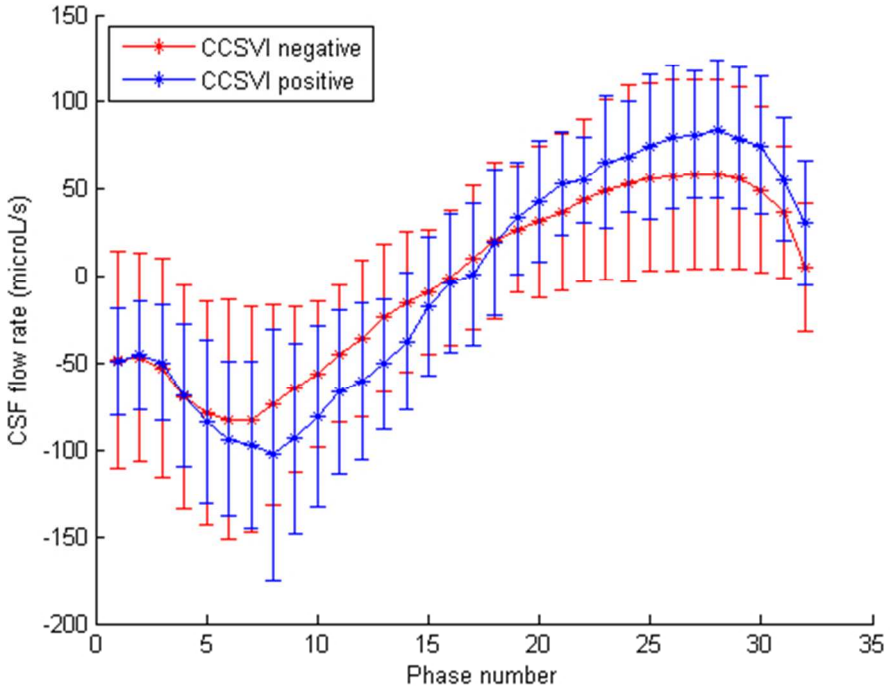

Figure 1. Ensemble mean aqueductal CSF flow signal over a cardiac cycle for both the CCSVI positive and negative groups. Between groups difference in positive amplitude (p=0.023) and negative amplitude (p=0.044). The phases of cycle where the difference between the signals is significant (p<0.050) are 8-14, 21 and 26-32. (Error bars represent one standard deviation.)
148x111mm (96 x 96 DPI)

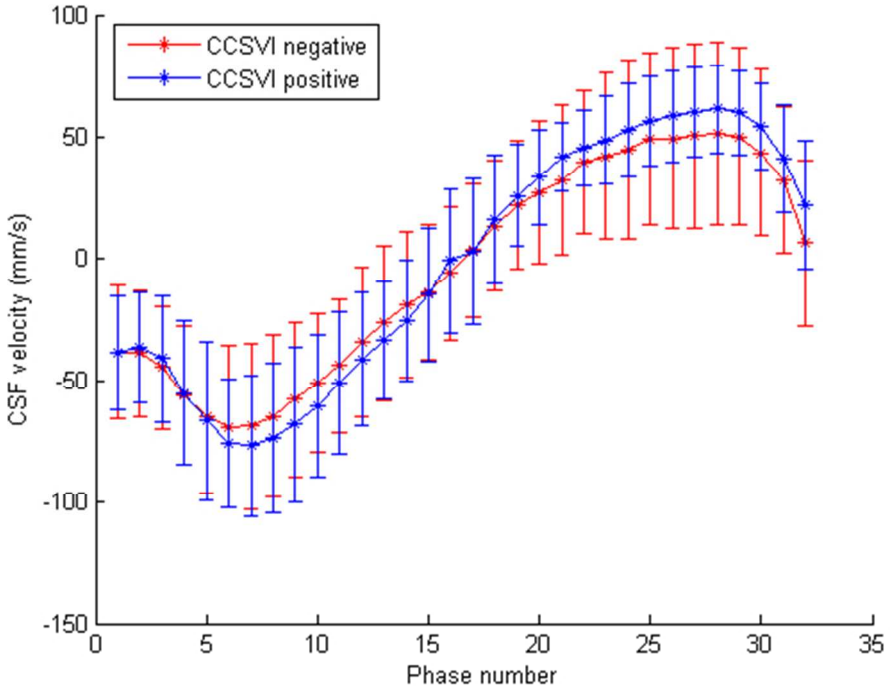

Figure 2. Ensemble mean aqueductal CSF velocity signal over a cardiac cycle for both the CCSVI positive and negative groups. Between groups difference in positive amplitude (p=0.136) and negative amplitude (p=0.316). A statistically significant difference between the signals (p<0.050) is only observed for phase 32 of the cycle. (Error bars represent one standard deviation.)
148x111mm (96 x 96 DPI)

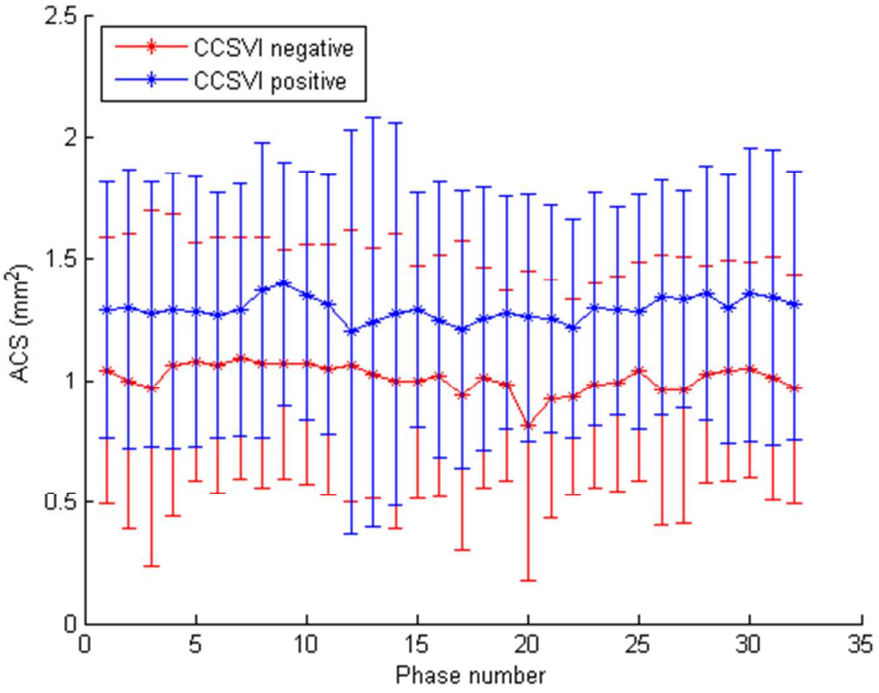

Figure 3. Sequential ensemble mean ACS over a cardiac cycle for both the CCSVI positive and negative groups. Between groups mean ACS, p=0.021. The phases of cycle where the difference between the signals is significant (p<0.050) are 8-10, 14-15, 18-28 and 30-32. (Error bars represent one standard deviation.)
148x111mm (96 x 96 DPI)

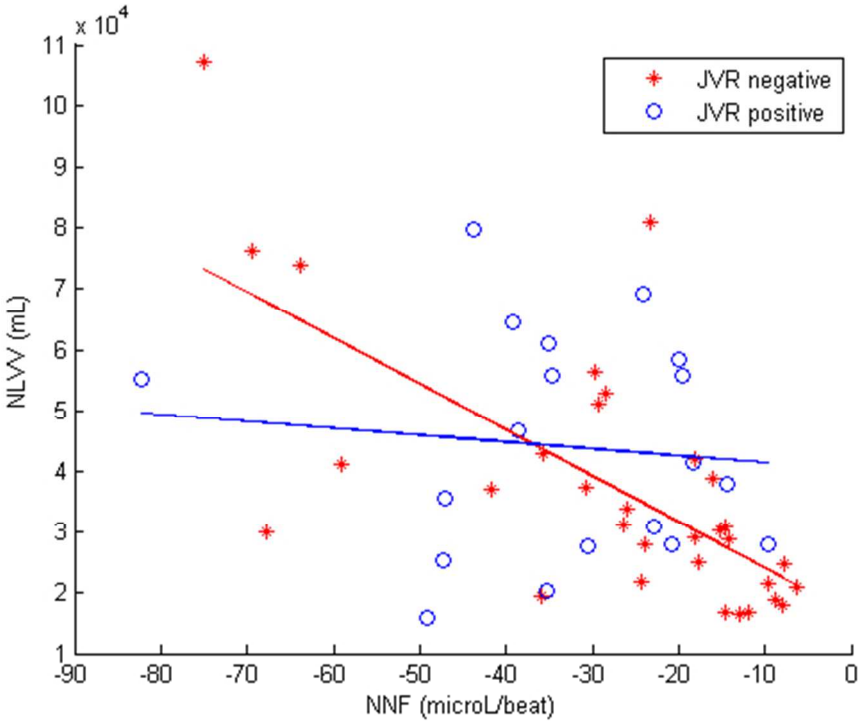

Figure 4. Scatter plot of NNF verses NLVV for the CCSVI positive and negative groups. CCSVI negative group (r=-0.686; p<0.001) and CCSVI positive group (r=-0.103; p=0.674).
148x111mm (96 x 96 DPI)

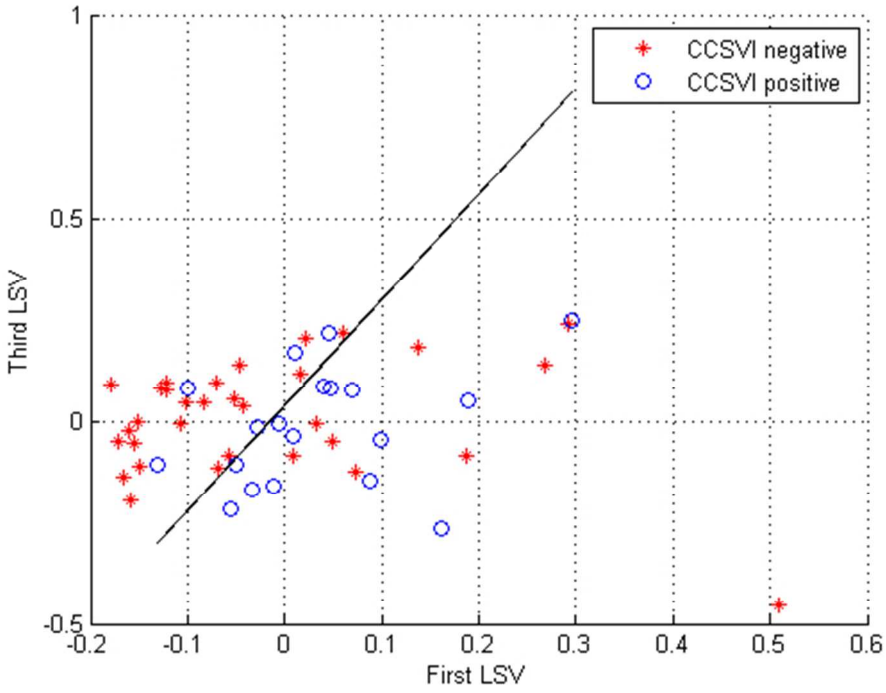

Figure 5. Singular value decomposition (SVD) cluster analysis results (derived using the three variables NNF, NPF and NLVV) (p=0.025).
148x111mm (96 x 96 DPI)